

# An Analytical Investigation of Steady Convection in an Active Mushy Layer

Prof. Dr. P.K.Srimani

Prof. R.Parthasarathi

*R & D Director (DSI), Former Chairman, B.U, Bangalore, Karnataka, INDIA*

*Professor and HOD, Dept. Mathematics, Jain University- CMS, Bangalore, Karnataka, INDIA*

**Abstract:** *In the present work, we consider the solidification of a binary alloy and analytically analyse the linear stability of the quiescent state by considering the basic, first and second order systems of the governing differential equations. The specific interest with which the study is carried out is to identify a model and the corresponding parametric values which could suppress the formation of chimney convection and annihilate the formation of freckles which cause imperfections in the resulting solid. The asymptotic limits considered here are a near-eutectic approximations, large far-field temperature and variable permeability. The consideration of large Stefan number incorporates a key balance for the existence of compositional convection. The important results of the present study are, (i) an active mushy layer is more stable than a passive mushy layer, (ii) the far-field temperature has a destabilising effect on the marginal stability curves as expected, (iii) there is a reduction in the mushy layer thickness for large far-field temperature, and (iv) the influence of the governing parameters is remarkable on the vertical velocity component, temperature and local solid fraction profiles. Finally it is concluded that, through an analytical approach it is possible to determine the accurate solutions which could control or suppress the chimney formation during the solidification process which is a burning problem in the areas like metal casting, sea dynamics etc. It is found that the results of the present study are very much closer to the experimental results,*

**Keywords:** *Mushy layer, Solidification, Compositional convection, Chimney formation, Variable permeability, Analytical.*

## I. INTRODUCTION

During the solidification process of binary or multicomponent alloys, the planar solidification front becomes morphologically unstable due to the constitutional undercooling which results in a mushy layer, the internal structure of which is composed of fine-scale crystals or dendrites through which the residual melt can flow. The interesting phenomenon observed at this stage is the occurrence of compositional convection. The driving force for this convection is the density gradient developed in the layer due to the rejected lighter component in the mixture. The dynamical behaviour of a mushy layer strongly depends on the complex interactions between the convection and the transfer of heat and solute which can remarkably modify the shape, structure and rate of the crystal growth. Accordingly, the distribution and the dissolution of the dendrites in the layer, induced by the convective process eventually lead

to the alteration of the permeability or the solid matrix of the mushy layer under consideration.

Convection in a mushy layer (also known as a dendritic layer) that is formed during the solidification of binary or multicomponent alloys, produces catastrophic effects on the crystal formed due to the formation of chimneys which are narrow, cylindrical dendrite free regions. The flow of fluid or convection in chimneys causes the hair – like imperfections called ‘freckles’ in the solid formed which are to be eliminated as they spoil the quality and the structure of the resulting crystal. The study of convection in a mushy layer has attracted several researchers during the past three decades. The main objective behind their study is to understand chimney convection and also to specify a model that can control or suppress the formation of freckles.

Especially in metallurgy, dynamics of sea and geophysics, the mechanism and the process of formation of chimneys which spoil the quality, physical properties and the internal structure of the resulting solid, are important study areas[1]-[3]. In the past three decades the study pertaining to the development of different convective models and analysis for the case of convection in mushy layers has attracted researchers [4],[5]. The works connected with the formulation of the governing equations in the study of convection in mushy layers, the development of mathematical models and the solution procedure are available[6],[7]. Linear and weakly nonlinear convective instability in a mushy layer have been studied by quite a number of researchers under different types of assumptions and approximations[7],[8] [9]-[13]. Quite a number of works on convective flow in a mushy layer is available. A detailed review on convection in mushy layers is given by [8],[14]. Recently [15]-[17] have applied weakly nonlinear evolution approach to study two-dimensional convective motions in a mushy layer with impermeable solidification front under different situations. Also [18] have studied numerically the effects of inertia on convection in a mushy layer with constant permeability. Experimentally a number of researchers [19],[1],[2],[20]-[25] have studied convection in mushy layers.

Further in the case of convection in a mushy layer under the external constraints, [26],[27] have studied compositional convection numerically under the influence of weak and strong vertical magnetic fields. The results predict that the chimney formation could be controlled in the presence of magnetic field. Numerically, [28] have studied the effect of variable permeability on convection in a mushy layer during the solidification

process in the presence and absence of an external magnetic field. For their computations they have considered large mushy layer thickness ( $\delta = 2$ ) and small for field temperature ( $\Theta_\infty = 0.1$  to  $0.3$ ). The results predict that convection in a mushy layer decreases with the increase in the magnetic field and increase in the far-field temperature. Recently [29],[30] have studied analytically the effects of inertia and permeability on the marginal stability curves and on the profiles of vertical velocity component, temperature, local solid fraction. The results are interesting. Thus the main objective of the present investigation is to have a good knowledge about the formation of chimney in a mushy layer during alloy solidification and present a model that could control or suppress the formation of chimneys so that the formation of freckles could be eliminated and the manufacturing process associated with the solidification process could be remarkably improved.

## II. MATHEMATICAL FORMULATION

The physical configuration consists of a horizontal mushy layer formed during the solidification of a binary alloy as shown in fig 1. The process of uniform cooling from below of the system results in the upward advancement of the solid – mush interface with a constant solidification speed  $V_0$ . In other words, the mushy layer is sandwiched between the solid and the liquid regions. The study is carried out in a moving frame of reference.

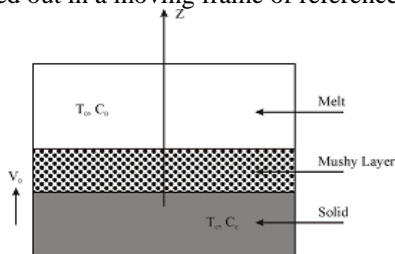


Fig. 1 The schematic diagram of the physical system

Following are the assumptions made for the study:

- i. The top and the bottom boundaries of the mushy layer are assumed to be isothermal, non-deformable and impermeable to the fluid flow, so that the mushy layer is kept dynamically isolated from the other components of the system [10].
- ii. The solidification front is moving upwards with a velocity  $V_0$  relative to the solid formed and the solid dendrites within the mushy layer. This makes the basic state to be steady.
- iii. The temperature  $T$  and the composition  $C$  of the liquid in the mushy layer are required to satisfy a linear liquidus relationship  $T = T_0(C_0) + \Gamma(C - C_0)$ , where  $\Gamma$  is a constant. The liquid is assumed to be Newtonian with a linearized equation of state  $\rho = \rho_0[1 + \beta(C - C_0)]$  where  $\rho$  is the density of the liquid and  $\rho_0$  is a reference density,  $\beta = \beta^* - \alpha$

$\Gamma$ ,  $\alpha$  and  $\beta^*$  are constant exponent coefficients for heat and solute respectively [31].

IV. First, following [10] we study in the limit in which the thickness of the mushy layer is much less than the diffusion length scale by letting  $\delta \leq 1$ .

V. However that a key implication of the near-eutectic approximations  $C = O(\delta^{-1})$  is that the solid fraction is small and hence the permeability is uniform to the lowest order. As a consequence, we follow [10] and expand the permeability in terms of the small solid fraction :

$$K(\Phi) = 1 + K_1(\Phi) + K_2(\Phi^2) + K_3(\Phi^3) + \dots \quad (1)$$

where on physical grounds, we demand that  $K_1, K_2, K_3, \dots$  etc are to be non-negative.

Under the above assumptions and approximations the governing equations of the system are Conservation of momentum, Conservation of mass, Conservation of heat and solute:

$$K(\Phi) \vec{q} + (\rho - \rho_0) \vec{g} \cdot \vec{k} + \nabla p = 0 \quad (2)$$

$$\nabla \cdot \vec{q} = 0 \quad (3)$$

$$\frac{\partial T}{\partial t} + (\vec{q} \cdot \nabla) T = k \nabla^2 T + \frac{l_h}{\gamma} \frac{\partial \Phi}{\partial t} \quad (4)$$

$$\chi \frac{\partial C}{\partial t} + (\vec{q} \cdot \nabla) C = (C - C_0) \frac{\partial \Phi}{\partial t} \quad (5)$$

where

$\Phi = 1 - \chi$  : Local solid fraction,  $\chi$  : Local liquid fraction,  $P$  : Dynamic pressure,  $\pi = \pi(\Phi)$ , permeability is a function of the local solid fraction,  $\mu$  : Dynamic

viscosity,  $t, T, k, l_h, \gamma$  are time, temperature, thermal diffusivity, specific heat, latent heat/unit mass,  $C_s$ : Composition of the solid phase,  $C_0$  : Composition of the liquid phase,  $\rho, \rho_0$  : densities,  $\vec{g} = (0,0,g)$  acceleration due to gravity,  $\pi(0)$  : The reference permeability,  $\vec{q} = u \vec{i} + v \vec{j} + w \vec{k}$ ,  $d$ : the mushy layer thickness,  $\vec{q}$  is the Darcy velocity vector and  $(u,v,w)$  are the horizontal and vertical components of  $\vec{q}$ ,  $\vec{i}, \vec{j}, \vec{k}$  : unit vectors along the  $x, y$  and  $z$  axes.

The boundary conditions are:

$$\begin{aligned} T &= T_e, w = 0 \text{ on } z = 0, \\ T &= T_0, w = 0, \Phi = 0 \text{ on } z = d. \end{aligned} \quad (6)$$

Here  $T_0$  is the temperature at the mush-liquid interface ( $z = d$ ) and  $T_s$  and  $C_s$  are the eutectic temperature and concentration at the mush-solid interface ( $z = 0$ ).

The dimensionless equations using the scales mentioned below are:

$$K(\Phi) \vec{q} + R \cdot \Theta \cdot \vec{k} + \nabla P = 0 \quad (7)$$

$$(\partial_t - \partial_z)(\theta - S\Phi) + (\vec{q} \cdot \nabla) \theta = \nabla^2 \theta, \quad (8)$$

$$(\hat{\partial}t - \hat{\partial}z) ((1 - \Phi) \theta + C \Phi) + (\vec{q} \nabla) \theta = 0, \quad (9)$$

$$\nabla \cdot \vec{q} = 0. \quad (10)$$

In this paper the case of variable permeability i.e.,  $K \neq 1$  is studied. The scales used for the non-dimensionalisation of the governing equations are

$$\begin{aligned} \vec{q} &= V_0 \vec{q}^* (\text{velocity}) \\ (x, y, z) &= \frac{k}{v_0} (x^*, y^*, z^*) (\text{length}) \\ t &= \frac{k}{v_0^2} t^* (\text{time}) \\ p &= \frac{k}{\mu \pi(0)} p^* (\text{pressure}) \\ K &= \frac{\pi(0)}{\pi(\theta)} \end{aligned} \quad (11)$$

The dimensionless parameters appearing in the problem are:

$$R = \frac{\beta \Delta C \pi(0) g}{\mu v_0} \text{ (Rayleigh number)}$$

$\beta$  is the volume expansion coefficient of the combined heat and solute [6].

$$S = \frac{l_h}{\gamma \Delta T} \text{ : Stefan Number}$$

$$C = \frac{C_0 - C_e}{\Delta C} \text{ : Concentration Ratio}$$

where

$$\Delta T = T_0 - T_e, \Delta C = C_0 - C_e, \pi(0) \text{ is the reference of } \pi$$

t: Time variable

$\Phi$ : Local solid fraction

**v : Kinematic viscosity**

$$\vec{V}_0 \text{ : Velocity of the solidification front} \quad (12)$$

$$\theta = \frac{T - T_0}{\Delta T} = \frac{C - C_0}{\Delta C} \text{ (The non-dimensional temperature or composition)}$$

The dimensionless boundary conditions are:

The non-dimensional boundary conditions at the upper boundary  $z = d$  correspond to an impermeable (rigid) flat boundary with zero solid fraction (i.e.,  $\varphi = 0$ ). Thus we have

$$\begin{aligned} \theta &= -1, w = 0 @ z = 0 \\ \theta &= 0, \varphi = 0, w = 0 @ z = \delta \end{aligned} \quad (13)$$

where  $\delta = \frac{d V_0}{K}$  is the growth pecllet number and also the dimensionless thickness of the mushy layer

### III. Method of solution

The method of solution constitutes two stages viz., basic state analysis and linear stability analysis. In the case of variable permeability,  $K$  is a function of porosity or the local solid fraction and is expressed as  $K(x, y, z, t) = \frac{\pi(0)}{\pi(\varphi)}$  which is similar to the Kozney-Carman relation [8]. The case of constant permeability corresponds to the decoupling of permeability and porosity. In that case

$$K(\varphi) = [1 - \varphi(x, y, z, t)]^n, n \neq 0 \quad (14)$$

In general the permeability function is considered as

$$(\Phi) = (1 - \Phi_b)^{-n}, n \neq 0 \quad (14a)$$

In the case of constant permeability,  $n = 0$  and  $K=1$ , While in the case of variable permeability,  $n = 3$ , so that

$$K(\Phi) = (1 - \Phi_b)^{-3} = \frac{1}{\chi^3} : \Phi = \Phi(z) \quad (14b)$$

The present study is for the case of variable permeability where  $n = 3$ . As discussed earlier, the physical configuration is such that it consists of a mushy layer, in which  $T_e$  is the eutectic temperature at which the lower mush – solid interface is maintained and  $T_\infty$  is the temperature of the liquid far above the mushy layer. Further  $T_0$  ( $C_0$ ) is the liquidus temperature of the alloy such that  $T_\infty > T_0$  ( $C_0$ ) and the mushy layer is assumed to be in a state of thermodynamic equilibrium so that

$$T = T_0(C_0) + \Gamma(C - C_0) \quad (15)$$

### IV. BASIC STATE ANALYSIS

The basic state corresponds to the steady motionless state

in which  $\vec{q} = 0$  and  $\frac{\partial}{\partial t} = 0$ . Thus we have the following set of equations:

Conservation of solute:

$$(1 - \Phi_b) D \theta_b + D \Phi_b (C - \theta_b) = 0 \quad (16)$$

Conservation of heat:

$$D^2 \theta_b + D \theta_b - S D \Phi_b = 0 \quad (17)$$

Conservation of momentum

$$\frac{d\Phi_b}{dz} - K \cdot \theta_b = 0 \quad (18)$$

The boundary conditions are

$$\theta_b = -1 @ z = 0$$

$$D \theta_b = \theta_\infty, \Phi_b = 0 @ z = \delta$$

(19)

Where,  $\theta_\infty$  is the far-field temperature. Here we take

$$\Phi_b = \delta \Phi_b, \theta_b = \theta_b \quad (20)$$

Substituting (19) in (15) and (16) we get

$$(1 - \delta \Phi_b) D \theta_b + \delta D \Phi_b (C - \theta_b) = 0$$

(21)

$$D^2 \theta_b + D \theta_b - \delta S D \Phi_b = 0 \quad (22)$$

Collecting the terms of  $O(\delta)$  and  $O(\delta)$  from (21) and (22) and solving the differential equations by using (19),

we get the basic state solutions as

$$\theta_b = (-1 + e^{\theta_\infty}) - e^{\theta_\infty} e^{-z} \quad (22a)$$

or

$$\theta_b = -1 + e^{\theta_\infty} - e^{\theta_\infty} (1+z),$$

so that

$$\theta_b = \theta_b = -1 + e^{\theta_\infty} z$$

Finally, we can write

$$\theta_b = C_1 + C_2 z \quad \text{and} \quad \Phi_b = C_3 + C_4 z \quad (22b)$$

where

$$C_1 = (-1 + e^{\theta_\infty}), C_2 = e^{\theta_\infty}, C_3 = -(C+S+1),$$

$$C_4 = e^{\theta_\infty}.$$

### V. LINEAR STABILITY ANALYSIS

As discussed earlier the analysis consists of two stages viz., the basic state analysis and the linear stability

analysis. For this purpose, we consider the expansion of the dependent variable  $\Theta$  and  $\Phi$  as

$$W(x,y,z,t) = 0 + \epsilon \hat{W}(x,y,z,t),$$

$$\hat{W} = (w_{00} + \delta w_{01})e^{(ikx + \sigma t)}$$

$$\theta(x,y,z,t) = \theta_{00} + \epsilon \hat{\theta}(x,y,z,t),$$

$$\hat{\theta} = (\theta_{00} + \delta \theta_{01})e^{(ikx + \sigma t)}$$

$$\Phi(x,y,z,t) = \Phi_b + \epsilon \hat{\phi}(x,y,z,t),$$

$$\hat{\phi} = (\phi_{00} + \delta \phi_{01})e^{(ikx + \sigma t)}$$

$$R = R_{00} + \delta R_{01} \tag{23}$$

where  $\epsilon$  is the perturbation parameter with  $\epsilon \ll 1$

and  $\hat{W}$ ,  $\hat{\theta}$  and  $\hat{\phi}$  are the perturbed quantities, which are expanded in terms of a small parameter  $\delta$ . Here  $k$  is the horizontal component of the wave number  $\alpha$  and  $\sigma$  is the growth rate of the disturbance. Further  $W_{00}$ ,  $W_{01}$ ,  $\theta_{00}$ ,  $\theta_{01}$ ,  $\phi_{00}$ ,  $\phi_{01}$  are purely functions of  $z$ . The basic state analysis has been performed in sec IV. Next from equations (6) to (9) and (23), the localized perturbed system is given by

$$K(\Phi) \cdot \vec{q} + \nabla \hat{P} + R \hat{\theta} \hat{k} = 0 \tag{24}$$

$$(\partial_t - \partial_z - \nabla^2) \hat{\theta} - S (\partial_t - \partial_z) \hat{\phi} + \hat{W} D \theta_b = 0 \tag{25}$$

$$(\partial_t - \partial_z) [(\theta_b - C) \Phi - (1 - \Phi_b) \hat{\theta}] - \hat{W} D \theta_b = 0 \tag{26}$$

together with the boundary conditions (27) and (28). The upper boundary i.e., mush-liquid interface is assumed to be flat and impermeable with zero solid fraction and whose temperature is equivalent to the liquidus temperature of the mushy layer as discussed earlier. Further the continuity of heat flux at the boundary is also assumed in order to facilitate the solution process. Mathematically, these are expressed as

$$\hat{W} = \hat{\theta} = 0 @ z = 0 \tag{27}$$

$$\hat{W} = \hat{\theta} = \hat{\phi} = 0 @ z = \delta$$

All the quantities have their predefined meanings (In all the future expressions, the ‘caps’ are dropped for the sake of simplicity). Next, we eliminate the pressure in (24), by applying curl twice and then consider the  $z$  - component of the equation for further analysis. In fact, the application of the transformation

$$\frac{\partial}{\partial z} \left[ \frac{\partial(it h)}{\partial x} + \frac{\partial(j t h)}{\partial y} \right] - \nabla_1^2(k t h) \tag{28}$$

on the momentum equation (in the component form) is same as that of applying curl twice and considering the  $z$ -component of the result. Now by using the following result, the resulting equations are obtained:

$$\nabla_x \nabla_x (K(\Phi) \vec{q}) \cdot \hat{k} = \frac{\partial}{\partial z} \left[ \frac{\partial(it h)}{\partial x} + \frac{\partial(j t h)}{\partial y} \right] - \nabla_1^2(k t h) \tag{28a}$$

Here, we are using the following results ;

$$\frac{\partial}{\partial z} \left[ \frac{\partial(K(\Phi)u)}{\partial x} + \frac{\partial(K(\Phi)v)}{\partial y} \right] - \nabla_1^2(K(\Phi) w) = \frac{\partial}{\partial z} [(1 - \Phi_b) - 3 \{u_x + v_y - \nabla_1^2 w\} - 3 (1 - \Phi_b) - 4 D \Phi_b D w] \tag{28b}$$

where  $D = \frac{d}{dz}$ . We write the resulting perturbed system as

$$\nabla_2 w + \frac{3D\phi_b}{(1-\phi_b)} D W - R \alpha^2 (1 - \Phi_b) \Theta = 0 \tag{29}$$

$$(\partial_t - \partial_z - \nabla_2) \theta - S ((\partial_t - \partial_z) \phi - (1 - \Phi_b) \theta) - D \theta_b w = 0 \tag{30}$$

$$(\partial_t - \partial_z) [(1 - \Phi_b) \theta - (\theta_b - C) \phi] + D \theta_b w = 0 \tag{31}$$

Now by using the expansion (23) through the normal mode approach for the physical variables, we write the system of order ( $\delta$ ) 0 as

$$\nabla_2 w_{00} + \frac{3}{(1 - \Phi_b)} D \Phi_b D w_{00} - R \alpha^2 \Theta_{00} (1 - \Phi_b) = 0 \tag{32}$$

$$(D^2 + D - \alpha^2 - \sigma) \theta_{00} - S (D - \sigma) \phi_{00} - D \theta_b W_{00} = 0 \tag{33}$$

$$(D - \sigma) [(\theta_b - C) \phi_{00} - (1 - \Phi_b) \theta_{00}] + D \theta_b W_{00} = 0 \tag{34}$$

The above system can be expressed as

$$L \alpha_{00} = 0$$

where  $\alpha_{00} = [w_{00}, \theta_{00}, \phi_{00}]^T$ ,  $T$  denotes the transpose and  $L$  is the linear operator given by

$$L = \begin{pmatrix} (D^2 - \alpha^2) + \frac{3D\phi_b}{(1-\phi_b)} \cdot D & -R_{00} \alpha^2 (1 - \phi_b)^3 & 0 \\ -D \theta_b & D^2 + D - \alpha^2 - \sigma & -S (D - \sigma) \\ D \phi_b & -(D - \sigma)(1 - \phi_b) + D \phi_b & (D - \sigma)(\theta_b - C) + D \theta_b \end{pmatrix} \tag{35}$$

By letting  $\Theta_{00} = -\sin \pi z$ , the solutions for the system (32) to (34) are given by

$$\phi_{00} = A_1 \sin \pi z + A_2 \cos \pi z + b_1(z) \tag{36}$$

$$w_{00} = A_1 \sin \pi z + A_2 \cos \pi z + b_2(z)$$

where

$$b_1(z) = A_2 \cdot z \text{ and } b_2(z) = A_2 (2z - 1)$$

$$A_1^* = \frac{[C + S + 1]}{(C + S + 1 - e^{\theta_{\infty}})}$$

$$A_2^* = \frac{-(\pi^2 + \alpha^2)}{\pi(C + S + 1 - e^{\theta_{\infty}})}$$

$$A_1 = \frac{\pi A_2^*}{e^{\theta_{\infty}}} [(e^{\theta_{\infty}} - C - 1)]$$

$$A_2 = \frac{-\pi}{e^{\theta_{\infty}}} [A_1^* (e^{\theta_{\infty}} - C - 1) + 1]$$

For the marginal stability  $\sigma = 0$  and by using the above results in (32), the expression for  $R_{00}$  is obtained:

$$R_{00} = \frac{(\pi^2 + \alpha^2) A_1}{\alpha^2} + \frac{3 \pi e^{\theta_{\infty}} A_2}{\alpha^2} \tag{37}$$

where  $\alpha$  is the wave number. Now in order to compute  $R = R_{00} + \delta R_{01}$ , we consider from (7) to (10) and (23), the system of order  $\delta$  as

$$(D^2 - \alpha^2) W_{01} + \frac{3D\phi_b}{(1-\phi_b)} D w_{01} - R_{01} \alpha^2 (1 - \Phi_b)^3 \Theta_{00} - R_{00} \alpha^2 (1 - \phi_b)^3 \theta_{01} - R_{00} \alpha^2 (1 - \phi_b)^3 \phi_{01} = 0 \tag{38}$$

$$(D2 + D - \alpha 2 - \sigma)\theta 01 - S(D - \sigma)\phi 01 - D\theta b W 01 = 0 \quad (39)$$

$$(D - \sigma)[(\theta b - C)\phi 01 - (1 - \phi_b)\theta 01] + D\theta b W 01 = 0 \quad (40)$$

By using the results of the first - order system and the solvability condition, the inhomogeneous equation (38) is solved for R01 in which the higher order effects appear. Thus we have

$$R01 = \frac{\frac{3\pi P_2 C_4}{4} [A_1^2 - A_2^2] - \frac{3P_2 R_{00}}{4} \alpha^2 (-A_1 + \frac{A_2}{\pi})}{\alpha^2 [\frac{A_1}{2} + \frac{3P_2}{4} (-A_1 + \frac{A_2}{\pi})]} \quad (41)$$

where, the other quantities have their predefined meanings. The critical value  $\alpha c$  corresponding to R00 is  $\pi$  and  $R0c = 2A1$ . Marginal stability curves for  $R = R00 + \delta R01$  are presented in fig.2 and 3 for the experimental values [21] of the parameters  $S = 3.2$ ,  $C = 9$ ,  $\theta\infty = 0.6, 0.7$  and  $\delta = 0.0, 0.03, 0.06$  respectively. The results are in excellent agreement with the numerical results of [28]. In order to study the effects of variable permeability on the vertical component of velocity  $w$ , temperature  $\Theta$  and the solid fraction  $\Phi$ , the second order system  $O(\delta)$  is solved by using the results of the basic state and the first order systems, with the computed value of R01 by solving the respective differential equations along with the boundary conditions. The following results are obtained:

$$w01 = C10 \sin \pi z + C11 \cos \pi z + b3(z) \quad (42)$$

$$\theta 01 = C12 \sin \pi z + C13 \cos \pi z + b4(z) \quad (43)$$

$$\phi 01 = C14 \sin \pi z + C15 \cos \pi z + b5(z) \quad (44)$$

where

$$P1 = 1, \quad P2 = e \theta\infty, \quad C1 = -(1 + e \theta\infty), \quad C2 = e \theta\infty, \quad C3 = -(C + S + 1), \quad C4 = e \theta\infty,$$

$$C5 = -\alpha 2 R01, \quad C6 = 0.$$

$$C7 = -[(\pi 2 + \alpha 2) C5 + \pi (1 - S) C6],$$

$$C8 = [-(\pi 2 + \alpha 2) C6 - \pi (1 - S) C5],$$

$$C9 = -\frac{[\alpha^2 R_{00} C_2 (e \theta\infty - c - s - 1)]}{(e \theta\infty - c - 1)},$$

$$C10 = \frac{[(C_{g1} + C_9) C_7 + \pi C_{g2} C_8]}{[C_{g1} + C_9]^2 + \pi^2 C_{g2}^2},$$

$$C11 = \frac{[(C_{g1} + C_9) C_8 + \pi C_{g2} C_7]}{[C_{g1} + C_9]^2 + \pi^2 C_{g2}^2},$$

$$C12 = \frac{[(C_5 + 3\pi C_4 C_{11}) + (\pi^2 + \alpha^2) C_{10}]}{-\alpha^2 R_{00}},$$

$$C13 = \frac{[(C_6 - 3\pi C_4 C_{10}) + (\pi^2 + \alpha^2) C_{11}]}{-\alpha^2 R_{00}},$$

$$C14 = \frac{[C_{12} - C_2 \frac{C_{11}}{\pi}]}{[e \theta\infty - c - 1]}, \quad C15 = \frac{[C_{13} + C_2 \frac{C_{10}}{\pi}]}{[e \theta\infty - c - 1]},$$

$$C91 = (\pi 2 + \alpha 2) 2 - 3C4 (1 - S) \pi 2,$$

$$C92 = -3C4 (\pi 2 + \alpha 2) - (\pi 2 + \alpha 2) (1 - S)$$

$$b3(z) = (2z - 1) C11, \quad b4(z) = (2z - 1) C13, \quad b5 = C15(z)$$

By using the above results the values of

$$w = w00 + \delta w01, \quad (45)$$

$$\Theta = \theta 00 + \delta \theta 01$$

$$(46)$$

$$\Phi = \phi 00 + \delta \phi 01 \quad (47)$$

are computed and the profiles are presented in figs.(4-9) and table 1 for the specified values of the parameters  $S, \theta\infty, C$  and  $\delta$ .

## VI. RESULTS AND DISCUSSION

As in the case of experimental studies, we consider in the present study an active mushy layer where the permeability is of variable type. The motivation for the present study is to achieve excellent agreement with the experimental results through an analytic approach. Another motivation for the present study is to present a model for convection in a mushy layer which could suppress the formation of freckles during the solidification process. As discussed earlier, the formation of freckles follows from chimney convection, and these cause imperfections in the structure as well as in the properties of the crystals formed. The governing equations considered under suitable assumptions and approximations are cast in the dimensionless form by using suitable scales. The mush-liquid interface is impervious and is under eutectic temperature. The solution process constitutes three stages.

In the first stage, basic state solutions are determined analytically by using the far-field temperature condition i.e.,  $D\theta b = \theta\infty$  @  $z = \delta$  at the upper boundary in addition to the other conditions. The solutions are extremely sensitive to the far-field temperature, Concentration ratio and the Stefan number. In the second stage, solutions ( $W00, \theta 00$  and  $\Phi 00$ ) to the linear stability system are found and the Rayleigh number R00 is found analytically and the critical wave number  $\alpha c = 5.1$ ,  $R0c = 31.69$  for  $\theta\infty = 0.6$  and  $R0c = 28.07$ ,  $\alpha c = 5.1$  for  $\theta\infty = 0.7$ ,  $S = 3.2$  and  $C = 9$  respectively. The computed results are presented through graphs in figs 2 and 3, for the above set of values of the parameters and  $\delta = 0.0, 0.03$  and  $0.06$  respectively. In fig 2, the graph of total  $R = R00 + \delta R01$  Vs the wave number  $\alpha$  is presented. It is found that the increase in the value of  $\delta$  decreases R. Further, R01 is determined from the higher - order inhomogeneous system of differential equations by applying the solvability conditions. The results are very much sensitive to the far-field temperature as expected. The results demonstrate that large  $\theta\infty$  enhances the values of  $w, \Theta$  and  $\Phi$  more significantly than a small value which is in consistency with the destabilising nature of the far-

field temperature on convection in an active mushy layer (Fig 3). In figs. 4-9 the profiles of  $w = w_{00} + \delta w_{01}$ ,  $\Theta = \Theta_{00} + \delta \Theta_{01}$  and  $\Phi = \Phi_{00} + \delta \Phi_{01}$  are presented for the above mentioned set of values.

The following observations are made; for all the computations the permeability function  $K$  is considered as a function of local solid fraction  $\Phi$  and the profiles indicate that (i) the vertical component of velocity is maximum at the middle of the layer (ii)  $w$  increases with  $\delta$  and the nonlinearity in the profile is more for large  $\delta$  (iii) there is a retardation in the velocity as  $\delta$  decreases (iv)  $\Theta$  is negative for all values of  $z$  (v) as  $\delta$  increases,  $\Theta$  increases in absolute value i.e. decreases. The nonlinearity is more pronounced as  $\delta$  increases and (vi) total  $\Phi$  is negative only in a restricted range i.e., near the bottom and is positive for all the other values. Even in this case, the nonlinearity of the profile increases with the increase in  $\delta$ . The results clearly show that, in the absence of inertia, there is a good amount of difference for the cases  $K=1$ (constant permeability) and  $K \neq 1$ (variable permeability) [3a]. The inhibition of convection in a mushy layer is possible by a proper choice of  $\Theta_{\infty}$  and the other parameters. The results are extremely sensitive to  $\Theta_{\infty}$  and the formation of freckles could be certainly be controlled which is a burning problem in metallurgy, geophysics etc. Finally it is concluded that our results are in excellent agreement with the experimental results of [1],[14],[21],[29]. It is evident that through the analytical approach it is possible to determine accurate solutions for convection in a mushy- layer although the model is quite complex.

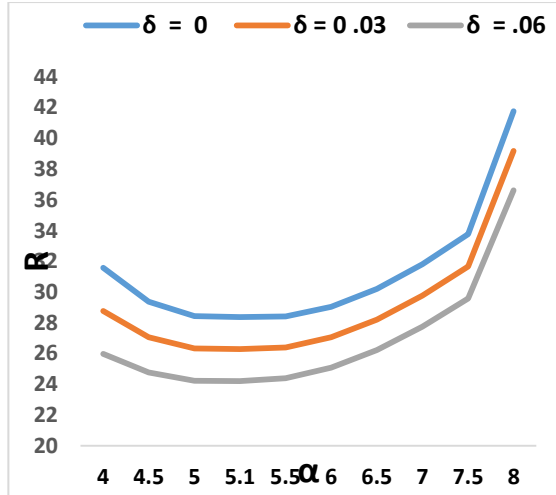


Fig. 3 Total R vs alpha for  $\delta = 0.0, 0.03, 0.06$  and  $\Theta_{\infty} = .7$

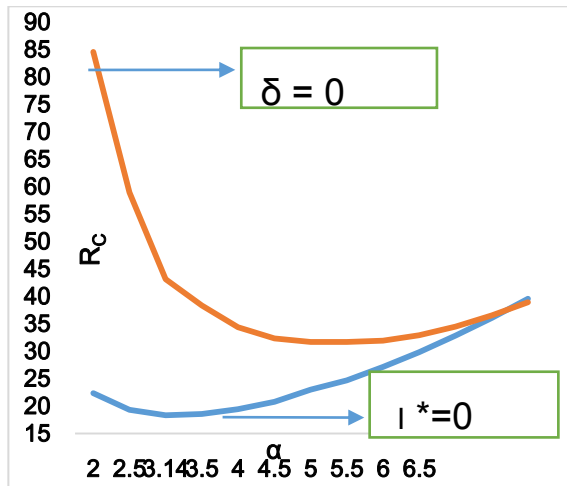


Fig.3a. Comparison graph of marginal Stability curves for:  $0.6, S = 3.2, C = 9$

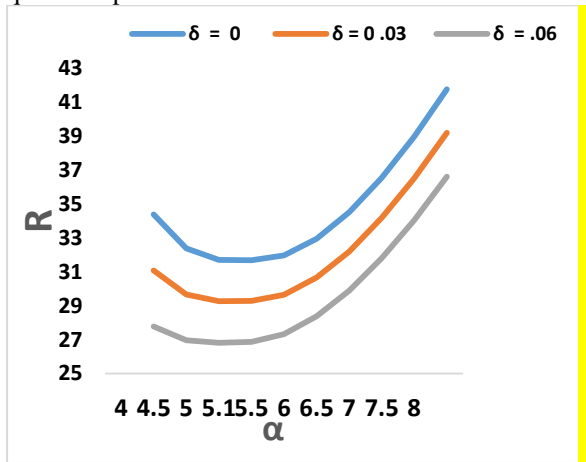


Fig.2 Total R vs alpha for  $\delta = 0.0, 0.03, 0.06$  and  $\Theta_{\infty} = .6$

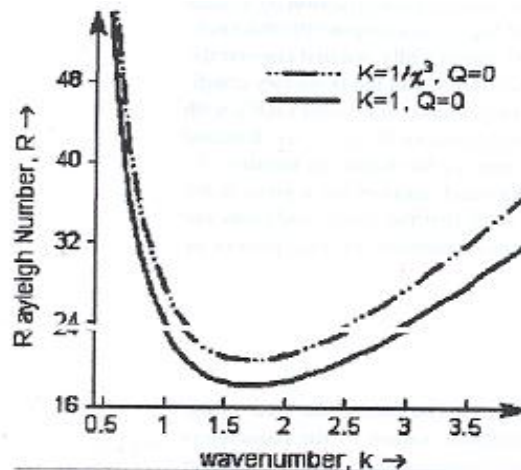


Fig. 3b Comparison graph of marginal stability curves[28]

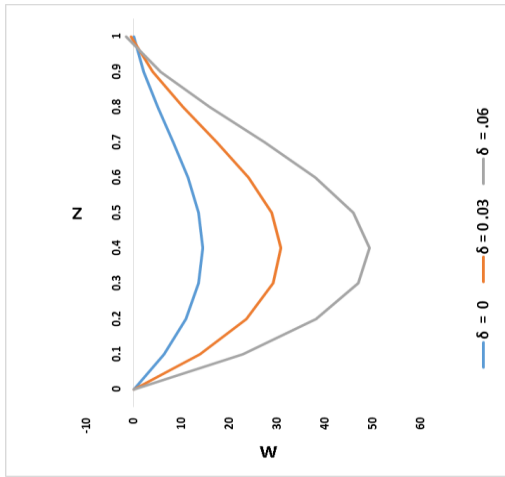


Fig. 4 Total W vs Z for  $\delta = 0.0, 0.03, 0.06$  and  $\Theta_{\infty} = .6$

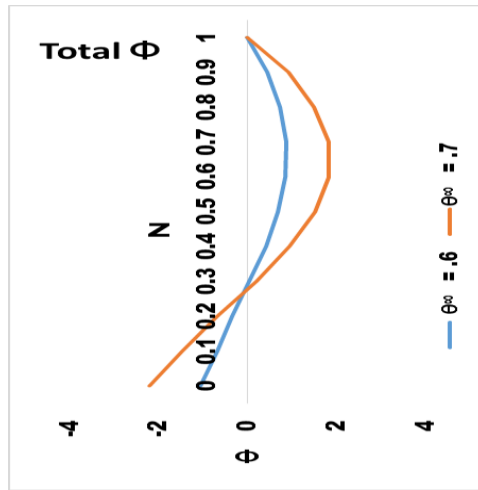


Fig. 7 Total  $\Phi$  vs Z for  $\delta = 0.03$  and  $\Theta_{\infty} = .6, \Theta_{\infty} = .7$

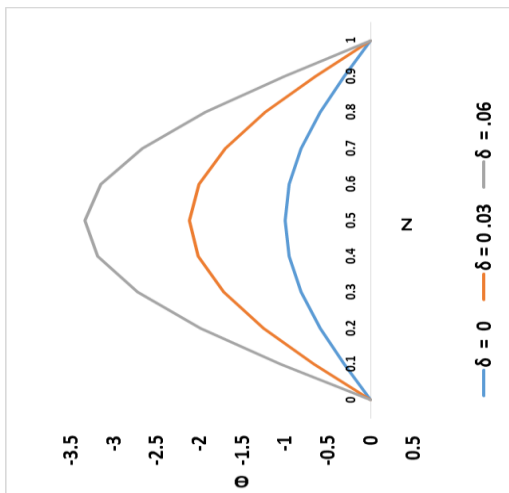


Fig. 5 Total  $\theta$  vs Z for  $\delta = 0.0, 0.03, 0.06$

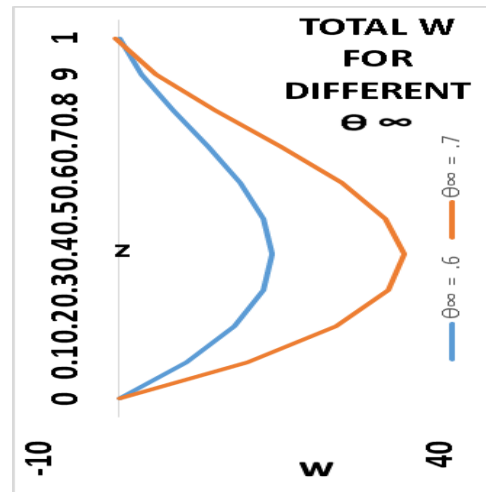


Fig. 8 Total W vs Z for  $\delta = 0.03$  and  $\Theta_{\infty} = .6, .7$

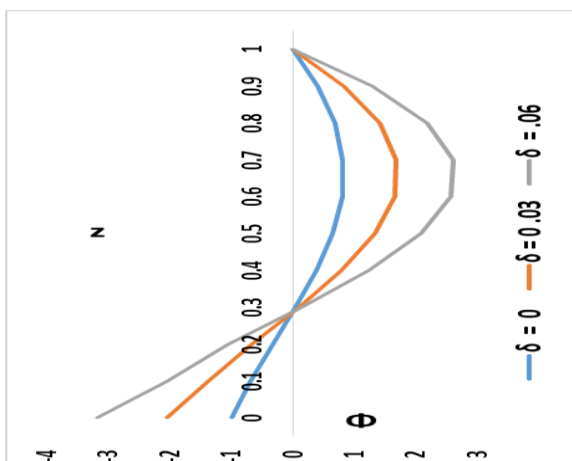


Fig. 6 Total  $\Phi$  vs Z for  $\delta = 0.0, 0.03, 0.06$

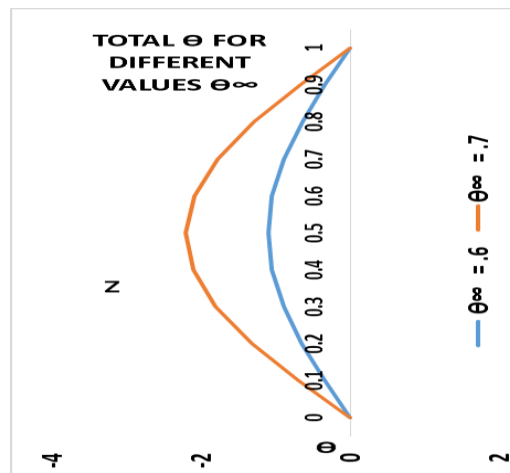


Fig. 9 Total  $\Theta$  vs Z for  $\delta = 0.03$  and  $\Theta_{\infty} = .6, .7$

## VII. ACKNOWLEDGEMENT

(R.P.) The author thanks the SCSVMV University, Kanchipuram(TN) and the Jain University, Bangalore, India, Vice Chancellor, Jain University and the Controller of Examinations, Jain University for providing the facilities and the encouragement to carry out this research work.

## VIII. CONCLUSION

During the past three decades, the theoretical as well as the experimental study of convection in a mushy layer has attracted a number of researchers owing to its wide applications in metallurgy, geophysics, Sea dynamics etc. The main objective behind these works is to reduce the formation of freckles which cause imperfections in the resulting solid during the alloy solidification. As discussed earlier, the distribution and dissolution of the dendrites in the layer induced by the convective process alter the permeability and the solid matrix of the mushy layer. Therefore, the present investigation was carried out in order to provide a model that could control or suppress the chimney formation during the solidification process.

The following conclusions are made:

(i) It is observed that the effect of variable permeability on the hydrodynamic convection in a mushy layer in the absence of inertia is of more stabilising nature than with the case of constant permeability [29]. In the absence of Inertia, the critical pair  $(\alpha C, R0c) = (5.1, 28.3754)$ , in the case of variable permeability, while for the case of constant permeability the critical pair  $(\alpha C, R0c) = (3.1416, 18.33746091)$ .

(ii) The remarkable results observed is that the far-field temperature  $\Theta_\infty$ , has a destabilising effect on the marginal stability curves as expected in all the cases.

(iii) Our results show that in the case of large far-field temperature, the mushy layer thickness  $\delta$  has to be small which is in conformity with the fact that, the heat flow from the liquid region to the mushy layer will be more when  $\Theta_\infty$ , is large and thus there will be a drastic reduction in the mushy layer thickness. This result is observed experimentally also [21].

(iv) The computed results (Figs 4 - 9) indicate that the vertical velocity is maximum at the middle of the layer and gradually proceeds towards the boundaries.

(v) The perturbed solid fraction is initially negative and then becomes positive.

(vi) Further the magnitude of the  $\Theta$  profile is less near the middle of the layer when compared to those near the boundaries.

(vii) Our analytical results demonstrate that an active mushy layer is more stable than a passive layer.

(viii) The results are extremely sensitive to  $\Theta_\infty$  and the formation of freckles could be certainly be controlled which is a burning problem in metallurgy, geophysics etc. Finally it is concluded that our results are very much closer to the experimental results of [1],[14],[29]. It is evident that through the analytical approach it is possible to determine accurate solutions for convection in a mushy- layer although the model is quite complex.

## REFERENCES

- [1] J.S. Wettlaufer, M.G.Worster, and H.E.Huppert, "The evolution of sea ice : solute trapping and brine-channel formation", J. Fluid Mech. vol.344, pp.291-316, 1997.
- [2] H.E.Huppert, and M.G. Worster, "Dynamic solidification of a binary melt, Nature", vol.314, pp. 703-707, 1985.
- [3] M. G. Worster, "Solidification of fluids. In Perspectives in fluid dynamics",(ed.G.K.Batchelor,H.K Moffatt, and M. G. Worster), pp.393-446, 2000.Camb.Univ.Press.
- [4] C.Beckermann, and C.Y.Wang, "Multiface Scale modelling of alloy solidification", Ann.Rev.Heat Transfer, vol. 6, pp.115-198, 1995.
- [5] T.P. Schulze, and M.G .Worster, "Weak convection, liquid inclusions and the formation of chimneys in mushy layers", J. Fluid Mech. vol. 388, pp.197-215, 1999.
- [6] R.N.Hills, D.E.Loper, and P.H.Roberts, "A thermodynamically consistent model of a mushy zone", Q.J.Mech.Appl.Maths, vol. 36, pp.505-539, 1983,
- [7] A.C.Fowler, "The formation of freckles in binary alloys", IMA J.Appl.Math. vol. 35, pp.159-174, 1985.
- [8] M. G. Worster, "Instabilities of the liquid and the mushy regions during solidification of alloys", J. Fluid Mech. vol. 237, pp.649-669, 1992.
- [9] C. A Chung, and F.Chen, "Onset of plume convection in mushy layers", J. Fluid. Mech, vol. 408, pp.53-82, 2000.
- [10] G.Amberg, and G.M.Homsy, "Nonlinear analysis of buoyant convection in binary Solidification with application to channel formation", J. Fluid Mech. vol. 252, pp.79-98, 1993.
- [11] D.M.Anderson, and M.G. Worster, "A new oscillatory instability in a mushy layer during the solidification of binary alloys", J. Fluid Mech. vol. 307, pp.245-267, 1996.
- [12] D.M.Anderson, and M.G. Worster, "Weekly nonlinear analysis of convection in mushy layers during the solidification of binary alloys", J. Fluid Mech. vol. 302, pp.307-331, 1995.
- [13] S.M.Roper, S.H.Davis, and P.W.Voorhees, "An analysis of convection in a mushy layer with a deformable permeable interface", J. Fluid Mech. vol. 596, pp.333-352, 2008.
- [14] M. G. Worster, "Convection in mushy layers", Annu. Rev. J. Fluid Mech. vol. 29, pp.91-122, 1997.
- [15] D.N. Riahi, "On nonlinear convection in mushy layers, Part 2. Mixed oscillatory and stationary modes of convection", J. Fluid Mech. vol. 517, pp.71-102, 2004.
- [16] D.N.Riahi, "On nonlinear convection in mushy layers, Part 1. Oscillatory modes of convection", J. Fluid Mech. vol. 467, pp.331-359, 2012.
- [17] D.N.Riahi, "On three dimensional non-linear buoyant convection in ternary solidification", Transp. Porous Med. vol. 103, pp.249-277, 2014.
- [18] D.Bhatta, D.N.Riahi, and M.S.Muddumallappa, "Inertial effect on convective flow in a passive mushy layer", J. Appl. Math. & Informatics, vol. 30, pp.499 – 510, 2012.
- [19] S.M.Copley, A.F.Giamei, S.M.Johnson, and M.F.Hornbecker, "The origin of freckles in uni - directionally solidified castings", metall.mater.Trans.I, vol. 1970, pp. 2193-2204.
- [20] M.G. Worster, "Solidification of an alloy from a cooled boundary, J. Fluid Mech". vol. 167, , pp.481-501, 198.
- [21] S.Tait and C.Jaupart, "Compositional convection in a reactive crystalline mush and melt differentiation", J.Geophys. Res. 97, pp.6735 - 6756, 1992.
- [22] F.Chen , J.W. Lu, and T.L.Yang, "Convective instability in ammonium chloride solution directionally solidified from below, J. Fluid Mech.", vol. 276, pp.163-187, 1994.

- [23] A.K.Sample, and A.Hellawell, "The mechanism of formation and prevention of channel segregation during alloy solidification", Metall.Trans.,15A, pp.2163-2173, 1984.
- [24] J.R.Sarazin, and A.Hellawell, "Channel formation in Pb-Sn, Pb-Sb, and Pb - Sn-Sb alloy ingots and comparison with the system NH<sub>4</sub>CL -H<sub>2</sub>O". Metall.Trans.19A, pp.1861-1871, 1988.
- [25] C.F.Chen, and F.Chen, "Experimental study of directional solidification of aqueous ammonium chloride solution", J. Fluid Mech.vol. 227, pp.567-586, 1991.
- [26] D.N.Riahi, "Effects of a vertical magnetic field on chimney convection in a mushy layer", J. Cryst. Growth , vol. 216, pp.501-511, 2000.
- [27] D.N.Riahi, "Effects of centrifugal and Coriolis forces on a hydromagnetic chimney convection in a mushy layer", J. Cryst. Growth, vol. 226, pp.393-405, 2001.
- [28] Dambaru Bhatta, S. Mallikarjunaiah, Muddumallappa, and Daniel N. Riahi, "On perturbation and marginal stability analysis of magneto - convection in active mushy layer", Transp. porous med., vol. 82, pp.385 - 399, 2010.
- [29] P.K. Srimani, and R.Parthasarathi, Inertial effects on hydrodynamic convection in a passive mushy layer, A.Int.J.Res.insci.Tech.Eng. & Math, 9(3), pp.221-229, 2015.
- [30] P.K.Srimani and R. Parthasarathi An Analytical Study of weakly Nonlinear Convection In a Horizontal Mushy layer, Int.J.E.Tech.Comp.App.Sci, 11(3), pp.239-246, 2015.
- [31] W.W.Mullins, and R.F.Sekerka, Stability of a planar interface during solidification of a binary alloy, J.Appl.Phys.35, pp.444-451, 1964.